IOPscience iopscience.iop.org

Home Search Collections Journals About Contact us My IOPscience

Assessment of operational space for long-pulse scenarios in ITER

This content has been downloaded from IOPscience. Please scroll down to see the full text.

2015 Nucl. Fusion 55 063019

(http://iopscience.iop.org/0029-5515/55/6/063019)

View the table of contents for this issue, or go to the journal homepage for more

Download details:

IP Address: 130.133.8.114
This content was downloaded on 13/05/2015 at 18:57

Please note that terms and conditions apply.

IOP Publishing | International Atomic Energy Agency Nuclear Fusion
Nucl. Fusion **55** (2015) 063019 (8pp) doi:10.1088/0029-5515/55/6/063019

Assessment of operational space for long-pulse scenarios in ITER

A.R. Polevoi[1], A. Loarte[1], N. Hayashi[2], H.S. Kim[3], S.H. Kim[1], F. Koechl[4], A.S. Kukushkin[1,5,6], V.M. Leonov[5], S.Yu. Medvedev[6,7], M. Murakami[8], Y.S. Na[3], A.Y. Pankin[9], J.M. Park[8], P.B. Snyder[8], J.A. Snipes[1], V.E. Zhogolev[5] and the IOS ITPA TG

[1] ITER Organization, Route de Vinon-sur-Verdon, CS 90 046, 13067 St Paul Lez Durance Cedex, France
[2] JAEA, Naka Fusion Institute, 801-1 Mukoyama, Naka-shi, Ibaraki-ken 311-0193, Japan
[3] Seoul National University, 1 Gwanak-ro, Gwanak-gu, Seoul 151-742, Republic of Korea
[4] Association EURATOM-ÖAW/ATI, Atominstitut, TU Wien, 1020 Vienna, Austria
[5] NRC 'Kurchatov Institute', Kurchatov sq. 1, 123098 Moscow, Russia
[6] NRNU MEPhI, Kashirskoye sh. 31, 115409 Moscow, Russia
[7] Keldysh Institute of Applied Mathematics, Miusskaya 4, 125047 Moscow, Russia
[8] General Atomics, 3550 General Atomics Court, San Diego, CA 92121, USA
[9] Tech-X Corp., 5621 Arapahoe Ave, Boulder, CO 80303, USA

E-mail: Alexei.Polevoi@iter.org

Received 18 December 2014, revised 30 March 2015
Accepted for publication 7 April 2015
Published 8 May 2015



Abstract

The operational space ($I_p - n$) for long-pulse scenarios ($\Delta t_{burn} \sim 1000$ s, $Q \geqslant 5$) of ITER has been assessed by 1.5D core transport modelling with pedestal parameters predicted by the EPED1 code by a set of transport codes under a joint activity carried out by the Integrated Operational Scenario ITPA group. The analyses include the majority of transport models (CDBM, GLF23, Bohm/gyroBohm (BgB), MMM7.1, MMM95, Weiland, scaling-based) presently used for interpretation of experiments and ITER predictions. The EPED1 code was modified to take into account boundary conditions predicted by SOLPS4 for ITER. In contrast to standard EPED1 assumptions, EPED1 with the SOLPS boundary conditions predicts no degradation of the pedestal pressure as density is reduced. Lowering the plasma density to $n_e \sim (5\text{–}6) \times 10^{19}$ m^{-3} leads to an increased plasma temperature (similar pedestal pressure), which reduces the loop voltage and increases the duration of the burn phase to $\Delta t_{burn} \sim 1000$ s with $Q \geqslant 5$ for $I_p \geqslant 13$ MA at moderate normalized pressure ($\beta_N \sim 2$). These ITER plasmas require the same level of additional heating power as the reference $Q = 10$ inductive scenario at 15 MA (33 MW NBI and 17–20 MW EC heating and current drive power). However, unlike the 'hybrid' scenarios considered previously, these H-mode plasmas do not require specially shaped q profiles nor improved confinement in the core for the transport models considered in this study. Thus, these medium density H-mode plasma scenarios with $I_p \geqslant 13$ MA present an attractive alternative to hybrid scenarios to achieve ITER's long-pulse $Q \geqslant 5$ scenario and deserve further analysis and experimental demonstration in present tokamaks.

Keywords: ITER, DT-phase, integrated modelling, long-pulse operation

(Some figures may appear in colour only in the online journal)

1. Introduction

Long-pulse operation with a current flat-top duration, $\Delta t_{burn} \sim 1000$ s at $Q = 5$ is foreseen in ITER to demonstrate tritium-concentration equilibrium scenarios that can be used for the qualification of nuclear technology and for assessing the test blanket modules (TBM). The main plasma regime foreseen for long-pulse $Q \geqslant 5$ operation is the hybrid scenario [1], which requires plasma confinement above the H-mode scaling but to a lesser extent than that required for the full steady-state ITER scenario ($\Delta t_{burn} \sim 3000$ s) [2]. Therefore, it is important to assess the viability of achieving ITER's long-pulse scenario goal ($\Delta t_{burn} \sim 1000$ s with $Q \geqslant 5$) with present-day transport models. The approach here is to forego special current profile shaping or artificial improvement of the core plasma energy confinement predicted by the transport models.

The operational space of long-pulse H-mode plasmas has been characterized for a range of plasma currents and plasma densities, determining the expected Q of these plasmas, by using 1.5D transport simulations and the correspondingly achievable burn length on the basis of the calculated flux consumption and the capabilities of the ITER PF system.

 © 2015 ITER Printed in the UK

Important inputs for the 1.5D transport simulations presented in this paper are the ITER pedestal plasma parameters, predicted using the EPED1 model [3–5], which is an approach widely used for integrated modelling of the ITER scenarios [6–10]. However, in contrast with previous studies, the EPED1 model was modified to take into account the expected differences in behaviour of the edge density in ITER compared to present experiments; namely: (a) that the fuelling of the pedestal plasma by neutrals is very inefficient, which breaks the link between separatrix density (n_{sep}) (controlled by neutral recycling and gas fuelling) and the pedestal density n_{ped} (controlled by pellet fuelling) and (b) that above a certain value of the neutral pressure at the divertor, n_{sep} saturates in ITER and does not increase anymore with divertor neutral pressure, as predicted by SOLPS simulations [7]. This behaviour is linked to the onset of divertor plasma detachment and strong plasma recombination. These two assumptions, when included in the EPED1 model for ITER H-mode plasmas with $n/n_G < 1$, lead to a pedestal pressure which is independent of pedestal plasma density in contrast to the EPED1 (with standard assumptions) predicted degradation of the pedestal pressure with the reduction of the pedestal density [3–8]. The difference between standard EPED1 predictions and EPED1 predictions that are consistent with SOLPS is discussed in section 2.

The possibility of long-pulse operation ($\Delta t_{burn} = 1000$–3000 s) with H-mode-like energy confinement ($H_{98(y,2)} \sim 1$–1.1) was already addressed earlier for the scaling-based model (SBM) [1, 2] in which core transport coefficients are adjusted to achieve a given H-factor. It was shown that high current operation $I_p \geqslant 13$ MA could achieve long-pulse $Q \sim 5$ plasma without the need to invoke energy confinement substantially above H-mode for the SBM model. In this paper, the core ITER plasma energy confinement has been evaluated by a range of transport models that successfully reproduce core plasma parameters in type I ELMy H-modes in present experiments. The sensitivity of the operational space of these long-pulse H-modes to the transport models used, namely: CDBM [10, 11], GLF23 [12], Bohm/gyroBohm (BgB) [13], MMM7.1 [14], MMM95 [15, 16], Weiland [17], Coppi–Tang [18], SBM [19, 20], is described in section 3.

Possible operational advantages and disadvantages of these low densities H-mode plasmas with respect to hybrid scenarios are discussed in section 4. The results of the studies described in this paper are summarized in section 5.

2. ITER pedestal predictions by EPED1

The EPED1 code is widely used in the integrated modelling of ITER scenarios, especially for long-pulse hybrid operation [6–8]. In present tokamaks, EPED1 [3–5] predictions of the pedestal height and width are relatively insensitive to separatrix conditions for most cases, and fixed values (referred further as standard) have been used for simplicity [3–5]:

$$T_s = 75\,\text{eV}, \qquad n_{ped}/n_s = 4, \tag{1}$$

for the hyperbolic tangential parametrization of the temperature and density profiles in the pedestal, $n(\psi) = n_s + \left(n_{ped} - n_s\right) F(\psi)/F1$, $T(\psi) = T_s + \left(T_{ped} - T_s\right) F(\psi)/F1$, where, ψ is the normalized poloidal magnetic flux, $F(\psi) = \tanh(1) - \tanh(2(\psi - \psi_{mid})/\Delta_{ped})$, Δ_{ped} is the pedestal width, $\psi_{mid} = 1 - \Delta_{ped}/2$, $\psi_{ped} = 1 - \Delta$, $F1 = \tanh(1) - \tanh(-1) \approx 1.5232$.

These assumptions are appropriate for present-day experiments in which the ionization of recycled neutrals provides the main particle source in the core plasma. They also provide an appropriate description of the pedestal plasma for the baseline ITER inductive 15 MA scenario with flat core plasma density profile, which requires a high pedestal density ($n_{ped} \sim n_G = 12 \times 10^{19}\,\text{m}^{-3}$) and strong pellet fuelling to reach $P_{fus} = 500$ MW with $Q = 10$.

In general, for ITER, the SOLPS predictions for the separatrix temperature and, most importantly, density in high power/high density scenarios required for fusion energy production, deviate substantially from the standard EPED1 assumptions in equation (1) because the neutral penetration into the core plasma is almost negligible in ITER. The link between n_s (determined mostly by the power outflow from the core and the need for divertor power load control and semi-detached divertor operation) and the pedestal density n_{ped} (controlled by pellet fuelling) is broken in ITER operational conditions, resulting in the saturation of the separatrix density and temperature at a given level that depends on the anomalous transport assumptions [9]. For a λ_q (heat flux e-folding length) of 3.6 mm in ITER these values are

$$n_s \sim (3-4) \times 10^{19}\,\text{m}^{-3}, \quad T_s \sim 0.2 - 0.3\,\text{keV}. \tag{2}$$

The temperature values at the pedestal, required for ITER H-mode operation, $T_{ped} \sim 3$–6 keV, are much higher than the separatrix values ($T_{ped} \gg T_s$). Thus, the standard EPED1 assumption, $T_s = 75$ eV does not affect edge stability in a significant way. The standard EPED1 assumption for density, $n_{ped}/n_s = 4$, is reasonable for the baseline $Q = 10$ scenario with a flat density profile and strong pellet fuelling. However, for moderate pedestal densities typical for the predicted long-pulse operation with flat core density profiles or for the baseline $Q = 10$ scenario with peaked density profile ($n_{ped} \sim 0.5 n_G$, $n_{ped}/n_s = 2$) which have lower pellet fuelling, a difference between the EPED1 predictions with standard assumptions (i.e. equation (1)) and those with the values in equation (2) is found.

The value of $\lambda_q = 3.6$ mm was chosen because this is the value for which the database of the SOLPS runs is the most extensive for ITER, which are the basis for the separatrix assumptions used in the modelling. Although recent experimental [21] and theoretical [22] studies would lead to a direct extrapolation for $\lambda_q \sim 1$ mm in ITER, this does not render the analysis presented in this paper invalid; in fact our results become a conservative lower limit for the Q that can be obtained in ITER in such conditions. As shown in [23], a decrease of λ_q leads to a higher density and temperature of the plasma at the separatrix for a given divertor peak heat flux (q_{div}) in ITER (where $q_{div} \leqslant 10\,\text{MW m}^{-2}$), which is favourable for fusion performance in the framework of the consideration presented in this paper. Indeed, the increase of the separatrix density to $n_s \sim (6$–$7) \times 10^{19}\,\text{m}^{-3}$ [24] for the same power crossing the separatrix (P_{SOL}) consistent with $\lambda_q \sim 1$ mm and $q_{div} < 10\,\text{MW m}^{-2}$ makes the density gradient in the pedestal lower and the temperature at the pedestal top higher than we

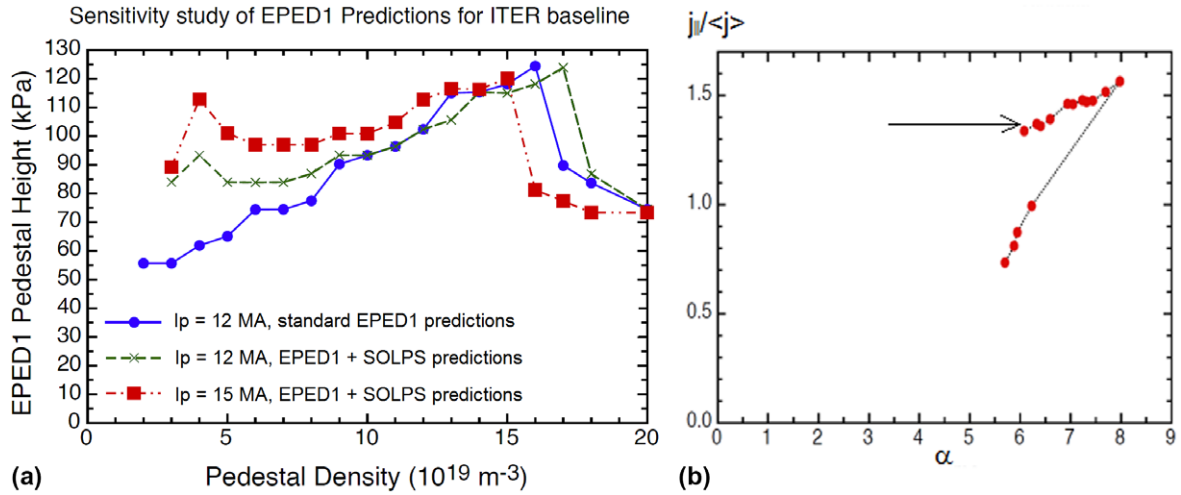


Figure 1. Pedestal parameters predicted by EPED1 for an ITER-like configuration: (*a*) pedestal height predicted by EPED1 with standard (12 MA) and SOLPS boundary conditions (15 MA, 12 MA); (*b*) stability diagram with standard assumptions at $I_p = 12$ MA, arrow shows the kink-peeling stability limit.

estimate with $\lambda_q \sim 3.6$ mm so that the fusion performance results obtained with $\lambda_q = 3.6$ mm are a conservative limit with respect to those achievable for $\lambda_q \sim 1$ mm. Note that with the reduction of the fusion power ($Q \sim 5$, figure 2) caused by the plasma density decrease to 5×10^{19} m^{-3}, the separatrix density drops below 5×10^{19} m^{-3}. Thus in principle a lower λ_q than 3.6 mm in ITER would not affect substantially the main conclusions of our study.

The results of EPED1 simulations for ITER with standard assumptions (equation (1)) can be fitted with accuracy ~5% by the following expression:

$$p_{\rm ped} \approx 2.55 B^{0.84} I_{\rm p} \left(0.32 + 0.36 n_{\rm ped}/n_{\rm G}\right) \text{ [kPa, T, MA]}. \quad (3)$$

Thus the pedestal pressure predicted for ITER by the EPED1 code with standard assumptions degrades almost linearly with a reduction of the pedestal density in the range below the Greenwald density, $n_{\rm ped} < n_{\rm G}$ (see circles in figure 1(*a*)), which can affect the plasma performance. For boundary conditions compatible with the SOLPS predictions (equation (2)) which have $n_{\rm ped}/n_{\rm s} < 4$, the pedestal pressure reduction with pedestal density is absent (see crosses and squares in figure 1(*a*)):

$$p_{\rm ped} \approx 1.7 B^{0.84} I_{\rm p} \text{ [kPa, T, MA]}. \quad (4)$$

For both assumptions the resulting pedestal width normalized to the poloidal flux can be fitted by

$$\Delta_{\rm ped} = 0.056 \left(p_{\rm ped}\right)^{0.5} / I_{\rm p} \text{ [kPa, MA]}. \quad (5)$$

The scalings (3)–(5) have a wide but finite range of applicability as the EPED1 results are calculated for the full bore ITER-like DT plasma with $a/R = 2/6.2$ [m/m], $\kappa_x = 1.88 - 1.85$, $\delta_x = 0.48$–0.485 in the range $q_{95} > 3$, $0.5 < n_{\rm eped}/n_{\rm GW} < 0.9$, $Z_{\rm eff} = 1.7$–2 in the scans with $\beta_{\rm N,tot} > 1.8$. Changes of shaping and excursion of plasma parameters beyond this range can make these scalings not applicable.

The appropriate values at the pedestal top correspond to

$$p_{\rm top} = 1.28 p_{\rm ped}, \qquad \Delta_{\rm top} = 1.5 \Delta_{\rm ped}. \quad (6)$$

The difference between the standard and modified EPED1 predictions can be explained by the strong dependence of the bootstrap current on the plasma density gradient. For the plasma density and temperature parametrization in the pedestal assumed in EPED1, the bootstrap current at the pedestal is the maximum possible, $j_{\rm max}/\langle j\rangle \sim j_{\rm bs,max}/\langle j\rangle$ (due to the aligned profiles of the temperature and the density in the pedestal). Thus, the pedestal height is at the kink-peeling stability limit (marked by arrow in figure 1(*b*)). Saturation of the separatrix density reduces the density gradient resulting in a reduction of the dominant contribution to the bootstrap current [25] for a given pressure gradient, $j_{\rm bs} \sim n'/n + 0.3T'/T$. As a result, the accessible pedestal pressure becomes higher than with the standard assumption, and the degradation of the pedestal pressure with decreasing pedestal densities disappears.

3. Operational space for long-pulse scenarios

An assessment of the operational space (OS) in terms of plasma current–plasma density for long-pulse operation in ITER DT plasmas has been carried out for a range $I_{\rm p} = 11$–15 MA, $n/n_{\rm G} = 0.5$–1 in plasma current and density respectively. Different transport models have been considered (CDBM, GLF23, Bohm/gyroBohm (BgB), MMM7.1, MMM95, Weiland, Coppi–Tang, scaling-based) for the study presented here. All models except the GLF23 provide a similar set of plasma parameters for the baseline ITER inductive DT operational point with $I_{\rm p} = 15$ MA, $P_{\rm fus} = 500$ MW, $Q = 10$, high density $n/n_{\rm G} \sim 1$ and burn duration $\Delta t_{\rm burn} \sim 400$ s. For implementation of the GLF23 model in the JINTRAC version used in the present simulations, the original torque diffusivity was replaced by $\chi_\phi = Pr\,\chi_i$ with $Pr = 0.5$, which predicts $Q = 7.5$ for the baseline scenario. A similar fusion gain, $Q = 10$ for the baseline scenario, is predicted by GLF23 with $Pr = 0.3$.

For the simulations in this study, we assume the same plasma heating and current drive (H&CD) with 33 MW of neutral beam injection (NBI) and 17–20 MW of electron cyclotron (EC) H&CD located at $r/a \sim 0.4$ of the minor

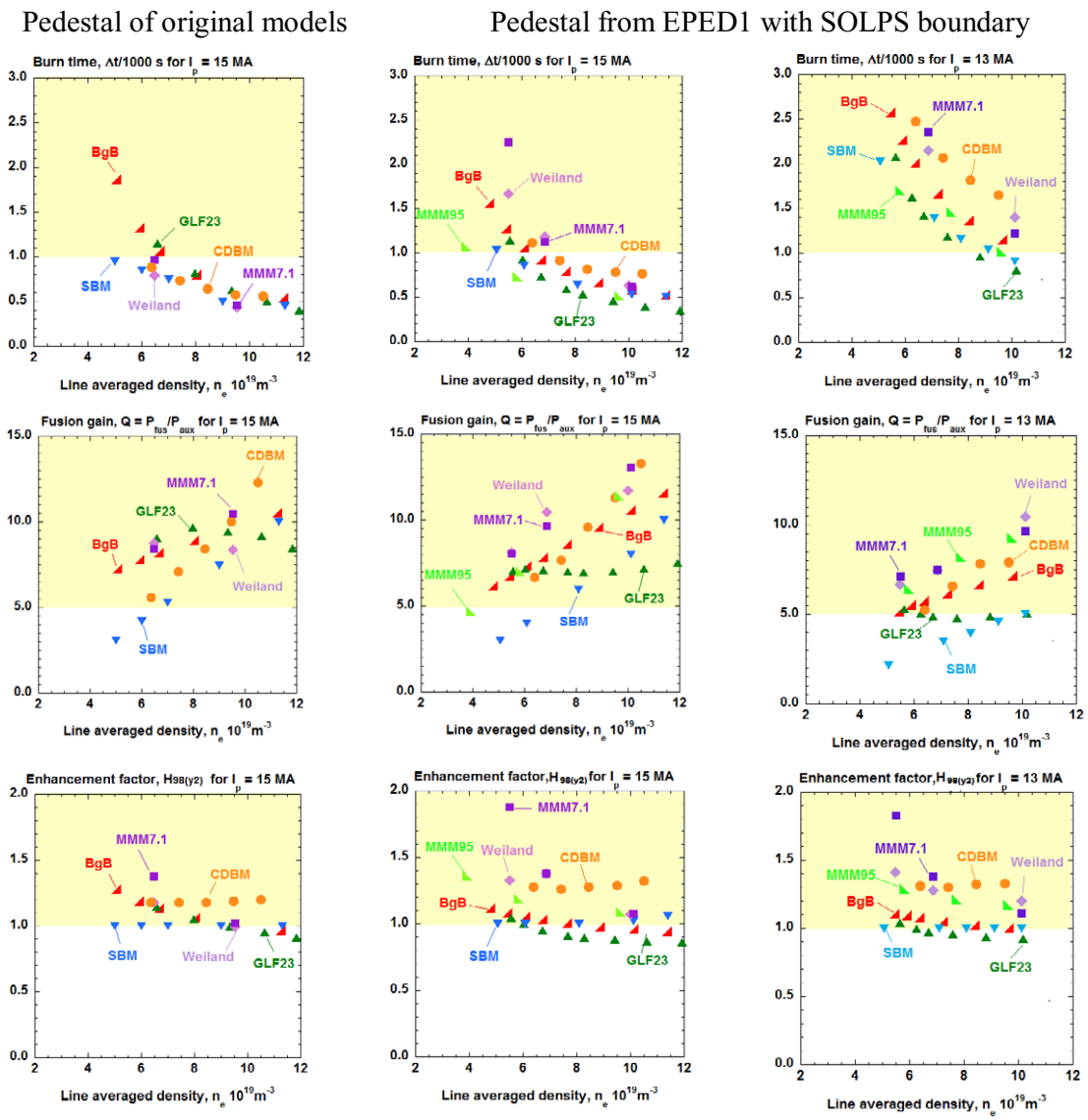


Figure 2. Burn time, Δt_{burn}, confinement enhancement factor, $H_{98(y,2)}$, fusion gain factor, Q, predicted by different core transport models for original implementation and for the EPED1 + SOLPS pedestal.

radius. For NBI, we consider one of the beams aimed at the innermost possible location and the other one at the outermost location. The plasma density at the pedestal top, n_{top}, is varied in the scan. The evolution of the plasma current density, the electron and ion temperatures and the density of the helium ash are calculated consistently with the 2D equilibrium. The beryllium and argon impurity concentrations are prescribed as fractions of the electron density, $n_{\mathrm{Be}}/n_{\mathrm{e}} = 2\%$, $n_{\mathrm{Ar}}/n_{\mathrm{e}} = 0.12\%$. The fuel density is calculated from quasi-neutrality assuming $n_{\mathrm{D}}/n_{\mathrm{T}} = 1$.

Two approaches have been taken in the study: in the first approach we use various transport models to assess the fusion gain and time of the burn phase achievable for a range of densities at $I_{\mathrm{p}} = 15$ MA keeping a constant pedestal pressure which provides the baseline operational point $Q \sim 10$ at $\langle n_{\mathrm{e}} \rangle \sim 0.9 n_{\mathrm{GW}}$ for the original implementation of each model. In general every transport model can require a different pedestal pressure assumption.

In the second approach we use a pedestal pressure consistent with EPED1+SOLPS predictions for all simulations together with the same transport models as for the first approach and we perform a plasma density scan for a range of plasma currents $I_{\mathrm{p}} = 11$–15 MA. In the pedestal area, the heat diffusivities are fitted to provide the temperature at the pedestal top and pedestal width, matching the EPED1+SOLPS predictions (equations (3)–(6)), which requires their reduction to typical values expected for ion neoclassical transport.

In both approaches for each model we kept the individual model assumptions on the transport of the fuel, helium ash, temperature, momentum, plasma current and on the saw-tooth oscillations following the model implementation in the corresponding code and used them for simulation of the baseline 15 MA ITER scenario. In both approaches the pedestal temperature increased along with the density reduction, $T_{\mathrm{ped}} \sim 1/n_{\mathrm{ped}}$, assuming constant pedestal pressure. Meanwhile the core temperature for each model changed individually according to the model predictions. The increase of the average electron temperature with the density reduction provides the increase of the flat-top length, $\Delta t \sim \langle T_{\mathrm{e}}^{3/2} \rangle$ (figure 2).

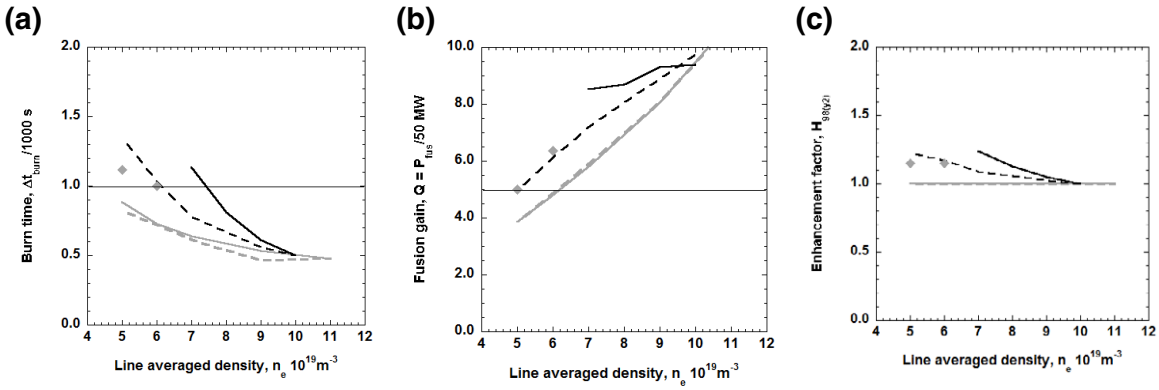


Figure 3. Predicted plasma performance for 15 MA inductive ITER scenarios with EPED1 pedestal for different densities for the SBM core transport model. The dashed lines correspond to the standard EPED1 predictions, the solid lines and diamonds correspond to EPED1+SOLPS predictions. Grey lines correspond to $H_{98(y,2)} = 1$, diamonds to $H_{98(y,2)} = 1.15$ and black lines to a stiff core transport model with, $T(0)/T_{\rm top} = \text{const}$.

In spite of the difference in the individual model assumptions, all of them predict a similar behaviour with the density reduction. The results of these simulations for burn length, $\Delta t_{\rm burn}$, confinement enhancement factor, $H_{98(y,2)}$, fusion gain factor, Q, normalized beta, $\beta_{\rm N}$, and H-mode quality, and $P_{\rm sol}/P_{\rm LH}$, are presented in figures 2 and 3 for 15 MA (original and EPED1+SOLPS model implementation) and 13 MA (EPED1+SOLPS model implementation). Here we use the following definitions: $\Delta t_{\rm burn} = (240 - 14I_{\rm p})I_{\rm p}/P_{\rm OH}$ [s, MA, MW], where $\Delta\Psi_{\rm burn} = 14I_{\rm p}$ [V s, MA] is the flux consumed during the current ramp-up, $\Delta\Psi_{\rm burn} = 240 - 14I_{\rm p}$ [V s, MA] the residual flux available for the current flat-top, $P_{\rm OH}$ is the ohmic power loss and $H_{H98(y,2)} = \tau_E/\tau_{H98(y,2)}$, where $\tau_{H98(y,2)}$ corresponds to the H-mode scaling [26] for the energy confinement time τ_E. $Q = P_{\rm fus}/P_{\rm aux}$, $\beta_{\rm N} = \beta aB/I_{\rm p}$ [%mT/MA] and $P_{\rm LH}$ corresponds to the L–H threshold scaling [27]. Note that in the confinement scaling on power, $\tau_{H98(y,2)} \sim P^{-0.69}$, we use $P = P_{\rm sol} = 0.2P_{\rm fus} + P_{\rm aux} + P_{\rm OH} - P_{\rm rad}$, where $P_{\rm rad}$ is the total radiation from the plasma core and $P_{\rm aux} = P_{\rm NB} + P_{\rm EC}$.

The results shown in figure 2 for the original model implementations demonstrate that for low density plasmas, $n_{\rm e} \sim 6\times10^{19}$ m^{-3}, a fusion gain $Q \geqslant 5$ with burn lengths of $\Delta t_{\rm burn} \geqslant 800$ s can be achieved with the usual H-mode energy confinement enhancement $H_{98(y,2)} \sim 1$ for all models even for a plasma current as high as $I_{\rm p} = 15$ MA.

The use of the new pedestal values predicted by EPED1+SOLPS can increase or degrade the expected plasma performance for the same level of $I_{\rm p}$ with respect to the original implementations of the various transport models. This is due to the fact that the pedestal pressure predicted by EPED1+SOLPS may be higher or lower than those used in the original implementation of the transport models, as shown in table 1.

For the pedestal plasma parameters predicted by EPED1 with the SOLPS boundary conditions, the lack of degradation of the pedestal pressure with reduced plasma density in ITER allows the achievement of the long-pulse $Q \geqslant 5$ scenario for standard core plasma H-mode transport assumptions for plasma currents in the range of $I_{\rm p} = 13$–15 MA resulting in $H_{98(y,2)} \sim 1$–1.3 energy confinement for the majority of the models. For the MMM7.1 model the plasma confinement increases more strongly with density reduction reaching values of up to $H_{98(y,2)} \sim 1.8$.

It is interesting to note that the pedestal height has a minor effect on predictions of the burn time and fusion gain for predictions with the scaling-based model. For the SBM, the effect of the increased pedestal temperature is balanced by the decrease of the core temperature required to keep the confinement $H_{98(y,2)} = 1$ which is assumed in this model.

To study the impact of the boundary conditions on plasma performance for different types of core transport we have performed a density scan for 15 MA plasma with flat density profiles and the SBM transport model for the top pedestal pressure from equations (3) and (4).

For each case we make two series of simulations, as shown in figure 3. In the first series, the core transport coefficients are fitted to provide the energy confinement time predicted for the H-mode operation, $\tau_E/\tau_{H98(y,2)} = H_{98(y,2)} = 1$ (lines) or 1.15 (diamonds). In the second one, we adjust the transport to provide $T(0)/T_{\rm top} \sim a/L_{\rm T} = \text{const}$ to simulate a stiff core transport. The simulations have been carried out for a range of average plasma densities, $n/n_{\rm G} = 0.5$–1 with 33 MW of the NBI heating and 17 MW of the EC heating.

These simulations show that the difference in the pedestal temperatures predicted by either standard EPED1 or EPED1+SOLPS has a negligible effect on the plasma performance for modelling by the SBM model with $H_{98(y,2)} = 1$ for 15 MA plasmas, because for this case the reduction of the pedestal temperature is compensated by the increase of the core temperature. It is worth noting that for $H_{98(y,2)} = 1$ the density reduction $n/n_{\rm G} \sim 0.5$ enables the increase of the flat-top duration to $\Delta t_{\rm burn} \sim 800$ s with $Q \sim 5$, as already found in [1, 2], providing an alternative to the hybrid scenario to achieve the ITER long-pulse (~1000 s) $Q = 5$ goal, which requires no improvement of the plasma confinement beyond the ITER H-98(y,2) scaling. A slightly better confinement ($H_{98(y,2)} \sim 1.15$) would allow increasing the flat-top duration to 1000 s with $Q > 5$ and increases the differences between the predictions done with the standard EPED1 model and those with EPED1+SOLPS for the lower densities, consistent with the higher pedestal temperatures and the increased core plasma fusion reactivity.

Table 1. Comparison of $p_{pe,mod}$ with the EPED1+SOLPS predictions for $I_p = 15$ MA.

Model Code	GLF23 [12] JINTRAC [28]	BgB [13] JINTRAC	SBM [20] ASTRA	MMM7.1 [14] ASTRA [29]	Weiland [17] ASTRA	CDBM [10] TOPICS [11]
$p_{pe,E+S}/p_{pe,mod}$	0.75	0.75	1.38	1.07	1.06	1.33

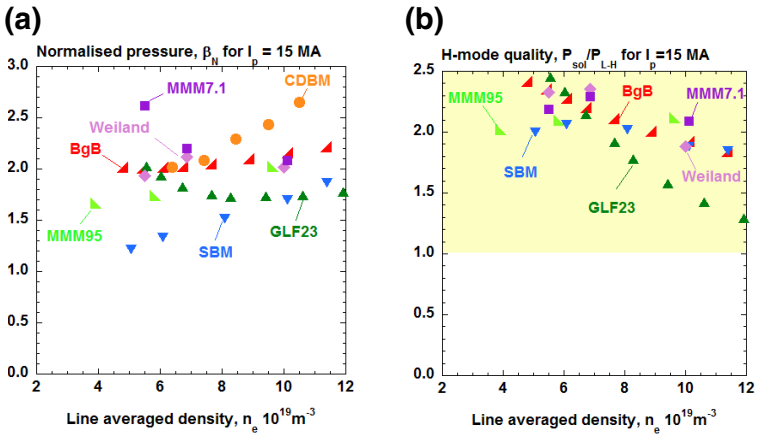


Figure 4. (*a*) Normalized beta, β_N, and (*b*) H-mode quality, P_{sol}/P_{LH}, predicted by different core transport models with the EPED1+ SOLPS pedestal for $I_p = 15$ MA.

As expected, the most pronounced effect of the SOLPS boundary conditions in EPED1 is obtained for the stiff core transport models given the direct correlation between the pedestal temperature and the central temperature. In particular, for the EPED1+SOLPS pedestal pressure (corresponding to higher temperature), the long-pulse operation with $\Delta t_{burn} \sim 1000$ s becomes possible at plasma density of 7×10^{19} m^{-3} with $Q \sim 8.5$, whereas for the standard EPED1, such a pulse length can only be reached at $n \sim 6 \times 10^{19}$ m^{-3} with $Q \sim 6.3$.

4. Possible advantages of lower density, high current operation

Operation at lower densities with high currents with H-mode like core transport has some additional advantages. Such operation has moderate normalized pressure, $\beta_N \sim 2$, (figure 4(*a*)), and an increased edge power margin above the L–H transition threshold, $P_{sol}/P_{LH} > 2$ (figure 4(*b*)).

They also have a potential for increased screening of tungsten in the pedestal because of the higher edge temperature and lower density gradients in the pedestal [31], and for a higher limit of the tungsten concentration acceptable for H-mode operation because of lower plasma densities, which has been quantified by detailed modelling studies.

An assessment of the maximum W density for good (H-mode) performance and of the effectiveness of the W influx crossing the separatrix to contaminate the core plasma has been carried out for ITER operation at 15 MA operation by 1.5D transport simulations with ZIMPUR [32] code in the ASTRA framework for the scaling-based model (core transport fitted to $H_{98(y,2)} = 1$) and pedestal transport fitted to the EPED1 + SOLPS predictions (equations (3)–(6)). As shown in figure 5, the weak dependence or the W radiation efficiency with temperature at high temperatures, leads to the total radiated power from the core plasma to be dominated by the plasma density ($P_{rad} \sim n_e^2 \times (n_W/n_e)$), which leads to a higher tolerable fraction of W for high performance H-mode operation at low densities in ITER.

Regarding W transport in these simulations we have considered two cases: one with purely anomalous tungsten transport, $D_w = D_{an} = (\chi_e + \chi_i)/10$ throughout the plasma including the edge transport barrier, and another one which includes neoclassical transport $V_p = V_{neo}$, $D_w = D_{an} + D_{neo}$. The effect of neoclassical transport is largest at the pedestal where density and temperature gradients are largest and leads to a reduced tungsten penetration for the low pedestal density/higher pedestal temperature plasmas due to the dominant temperature screening. For all simulations a given W influx a radial W velocity of 1 m s^{-1} is assumed at the separatrix and the value of the influx has been adjusted until the core W concentration reaches the maximum allowed value in figure 5. As shown in figure 6, for the low density H-modes the large pedestal temperature gradients provide a very effective neoclassical screening of the W compared to a purely diffusive model and W fluxes up to a factor of 4 larger are found to be acceptable regarding W contamination of the core plasma. At high densities this effect is smaller given larger density gradients and lower temperature gradients in the pedestal which make the temperature screening less efficient. In this sense low core density H-mode operation with no or low pellet fuelling with comparable separatrix densities to those of 15 MA $Q \sim 10$ conditions are more resilient to contamination of the core plasma by W produced at the divertor.

The low density, high current H-modes are also less demanding with regards to core fuelling requirements that is provided by pellet injection in ITER.

The total HFS pellet injection rate, G_{HFS}, required to achieve a given pedestal density has been estimated using the effective transport coefficients derived from the separatrix parameters, predicted by SOLPS [33] and pedestal top parameters predicted by equations (3)–(6), assuming $D = \chi_{eff}/10$. From equations (3)–(6) the heat diffusivity can

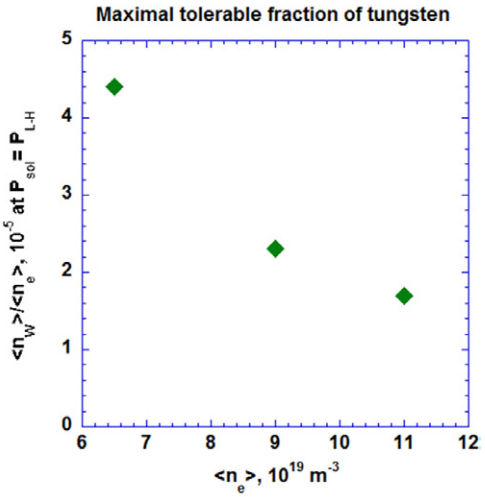


Figure 5. Maximal fraction of tungsten for 15 MA scenario tolerable for H-mode operation.

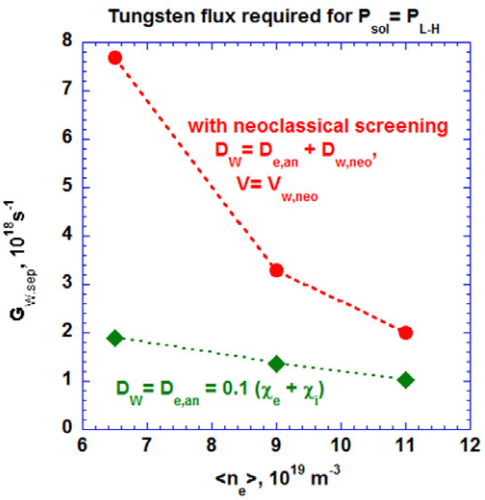


Figure 6. Maximal tungsten flux allowed the H-mode operation for $I_p = 15$ MA with the SBM.

be expressed as a function of the power outflow to the SOL, $\chi_{\rm eff} \approx 2P_{\rm SOL}\Delta_{\rm top}/S_a p_{\rm top}$, where $P_{\rm SOL}$ is the power crossing the separatrix, $\Delta_{\rm top}$ is the distance between the separatrix and the pedestal top, $p_{\rm top}$ is the plasma pressure at the pedestal top and S_a is the plasma surface area.

The particle flux across the separatrix is thus given by $G_{\rm SOL} = S_a D\nabla n \approx P_{\rm sol}\left(n_{\rm top} - n_{\rm s}\right)/\left(5p_{\rm top}\right)$. Given the low efficiency of neutrals to fuel the core plasma $G_{\rm SOL}$ has to be provided by pellet injection from the high field side (HFS) in ITER. The reduction of plasma density reduces the particle diffusive loss, $G_{\rm SOL}$ by a factor of 5 (figure 7). The required HFS pellet fuelling should be higher to compensate the controlled ELM-driven particle loss. The HFS pellet injection rate required for core fuelling including LFS pellet injection for ELM control [34, 35] and divertor control is also shown in figure 7. These calculations were done for a controlled ELM loss of $\Delta W_{\rm ELM} = 0.6$ MW, and a LFS pellet size for ELM triggering of $N_{\rm pel} \sim 3.7\,{\rm Pa\,m^3}$, assuming a flat density profile, for the scalings of the particle fluxes, total particle throughput and separatrix density derived in [33]

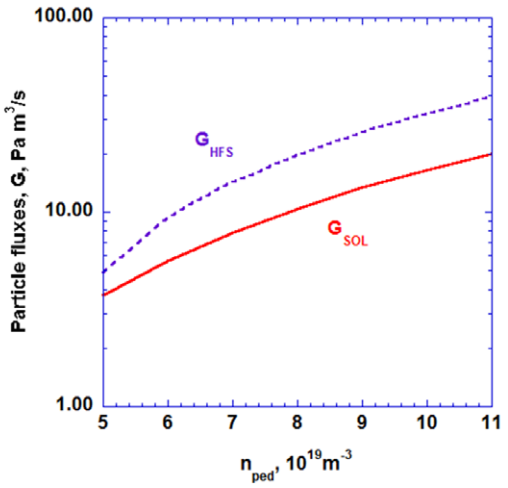


Figure 7. Particle outflux, $G_{\rm SOL}$ and required core fuelling by pellets, $G_{\rm HFS}$, for $I_p = 15$ with EPED1+SOLPS pedestal for $P_{\rm SOL}/P_{\rm LH} = 1.4$.

(more details of this evaluation will be published elsewhere). This assessment shows that the reduction of H-mode operating density from 11 to $5 \times 10^{19}\,{\rm m^{-3}}$ leads to a reduction of the required fuelling rate by HFS pellets by a factor of eight.

5. Summary and conclusions

The EPED1 model with boundary conditions from SOLPS predicts no degradation of pedestal pressure with decreasing pedestal density in ITER. In general, this requires a reassessment of the integrated modelling results which assume a low ratio of pedestal to separatrix densities ($n_{\rm ped}/n_{\rm s} < 4$) in simulations with stiff core transport but utilize the pedestal pressure predicted by EPED1 with the standard assumptions [4–6]. Such simulations are very sensitive to the assumptions regarding the pedestal height [30].

Modelling of core transport with 1.5D transport models carried out with pedestal parameters predicted by EPED1+SOLPS indicates that there is a large operational space for the long-pulse plasma operation with a high fusion gain $Q \geqslant 5$. Reducing the plasma density to $n_{\rm e} \sim (5\text{–}6) \times 10^{19}\,{\rm m^{-3}}$ leads to an increased pedestal plasma temperature due to the pedestal pressure being the same at low and high densities in these ITER conditions. This reduces the loop voltage and increases the duration of the burn phase to $\Delta t_{\rm burn} \sim 1000$ s with $Q \geqslant 5$ for $I_p \geqslant 13$ MA at moderate normalizsed pressure ($\beta_N \sim 2$). These ITER plasmas require the same level of additional heating power as the reference $Q = 10$ inductive scenario at 15 MA (33 MW NBI and 17–20 MW EC heating and current drive power). Unlike the 'hybrid' scenarios considered previously, these H-mode plasmas require no specially shaped q profiles or improved confinement in the core for the majority of the transport models considered in this study. In particular, for the scaling-based transport model with constant $H_{98(y,2)}$, the increase of the pedestal temperature due to the new pedestal pressure values from EPED1 with SOLPS boundary conditions is mostly compensated by the reduction of the core temperature. Thus, the pedestal height has a minor effect on the predictions of the burn time and fusion gain by the scaling-based model.

Such operation has moderate normalized pressure ($\beta_N \sim 2$), increased edge power margin above the L–H transition threshold, $P_{sol}/P_{LH} > 2$, better screening of tungsten in the pedestal due to more favourable pedestal transport, and a higher limit of the tungsten concentration acceptable for H-mode operation due to the lower density. It is also less demanding for core fuelling and keeps fusion power and divertor loads at moderate levels for potential temperature excursions up to the MHD limit ($\beta_N = 4l_{i1}$) due to the large increase of plasma temperature in these conditions ($T_e(0) \sim T_i(0) > 35$ keV) which prevents the alpha heating power from increasing as β_N increases and leads to a significant increase of the power lost by the plasma by electron cyclotron radiation [36]. The new assumptions on the separatrix plasma parameters consistent with SOLPS do not affect the ITER reference scenario for $Q = 10$ ($I_p = 15$ MA with $n/n_G \sim 1$) with respect to fusion performance and pulse length for flat density profiles ($n_{ped} \sim n$) previously modelled using the pedestal parameters predicted by the EPED1 code with standard assumptions.

We can therefore conclude that medium density H-mode plasma scenarios with $I_p \geqslant 13$ MA present an attractive alternative to hybrid scenarios to achieve ITER's long-pulse $Q \geqslant 5$ and deserve further analysis and experimental demonstration in present tokamaks.

Acknowledgments

The authors express their acknowledgements to D.J. Campbell, T.C. Luce, A.C.C. Sips, S. Ide for support of this work and useful discussions.

The views and opinions expressed herein do not necessarily reflect those of the ITER Organization.

References

[1] Luce T.C. *et al* 2014 *Nucl. Fusion* **54** 013015
[2] Polevoi A.R. *et al* 2010 *37th EPS Plasma Physics Conf. (Dublin, Ireland, 2010)* P2.187 http://ocs.ciemat.es/EPS2010ABS/pdf/P2.187.pdf
[3] Snyder P.B. *et al* 2004 *Plasma Phys. Control. Fusion* **46** A131
[4] Snyder P.B. *et al* 2011 *Nucl. Fusion* **51** 103016
[5] Snyder P.B. *et al* 2012 *Phys. Plasmas* **19** 056115
[6] Citrin J. *et al* 2010 *Nucl. Fusion* **50** 115007
[7] Kim S.H. *et al* 2012 CORSICA modelling of ITER hybrid mode operation *24th Int. Conf. on Fusion Energy (San Diego, CA, 2012)* www-naweb.iaea.org/napc/physics/FEC/FEC2012/papers/236_ITRP113.pdf
[8] Litaudon X. *et al* 2013 *Nucl. Fusion* **53** 083012
[9] Pacher H.D. *et al* 2011 *J. Nucl. Mater.* **415** S492
[10] Garcia J. *et al* 2012 *Proc. 39th EPS Conf. on Controlled Fusion and Plasma Physics (Stockholm, Sweden, 2012)* P5.057 http://ocs.ciemat.es/epsicpp2012abs/pdf/P5.057.pdf
[11] Hayashi N. and the JT-60 Team 2010 *Phys. Plasmas* **17** 056112
[12] Waltz R.E. 1997 *Phys. Plasmas* **4** 2482
[13] Erba M. *et al* 1997 *Plasma Phys. Control. Fusion* **39** 261
[14] Rafiq T. *et al* 2011 *Phys. Plasmas* **18** 112608
[15] Bateman G. *et al* 1998 *Phys. Plasmas* **5** 1793
[16] Na Y.-S. *et al* 2009 *Nucl. Fusion* **49** 115018
[17] Weiland J. *et al* 2009 *Nucl. Fusion* **49** 065033
[18] Crotinger J.A. *et al* 1997 *LLNL Report* UCRL-ID-126284; *NTIS* #PB2005-102154
[19] Polevoi A.R. *et al* 2006 *Plasma Phys. Control. Fusion* **48** A449
[20] Leonov V.M. and Zhogolev V.E. 2012 *39th EPS Conf. (Stockholm, Sweden, 2012)* P5.009 http://ocs.ciemat.es/epsicpp2012abs/pdf/P5.009.pdf
[21] Eich T. *et al* 2013 *Nucl. Fusion* **53** 093031
[22] Goldston R.J. 2012 *Nucl. Fusion* **52** 013009
[23] Kukushkin A.S. *et al* 2013 *J. Nucl. Mater.* **438** S203
[24] Kukushkin A.S. *et al* 2013 *Nucl. Fusion* **53** 123024
[25] Sauter O. *et al* 1999 *Phys. Plasmas* **6** 2834–9
[26] ITER Physics Basis 1999 *Nucl. Fusion* **39** 2208
[27] Martin Y.R. *et al* 2008 *J. Phys.: Conf. Ser.* **123** 012033
[28] Romanelli M. *et al* 2014 *Plasma Fusion Res.* **9** 3403023
[29] Pereverzev G.V. and Yushmanov P.N. 2002 ASTRA automated system for transport analysis *IPP-Report* IPP 5/98
[30] Mukhovatov V. *et al* 2003 *Nucl. Fusion* **43** 942
[31] Dux R. *et al* 2014 *Plasma Phys. Control. Fusion* **56** 124003
[32] Leonov V.M. and Zhogolev V.E. 2005 *Plasma Phys. Control. Fusion* **47** 903
[33] Pacher H.D. *et al* 2015 Impurity seeding in ITER DT plasmas in a carbon-free environment *J. Nucl. Mater.* in press (http://dx.doi.org/10.1016/j.jnucmat.2014.11.104)
[34] Polevoi A.R. *et al* 2008 *Proc. 35th EPS Conf. on Controlled Fusion and Plasma Physics (Hersonissos, Greece, 2008)* P1.109
[35] Kukushkin A.S. *et al* 2011 *J. Nucl. Mater.* **415** S497–500
[36] Kukushkin A.B. *et al* 2011 *38th EPS Conf. on Plasma Physics (Strasbourg, France, 27 June–1 July 2011)* P4.072 http://ocs.ciemat.es/EPS2011ABS/pdf/P4.072.pdf